Sensing methanol concentration in direct methanol fuel cell with total harmonic distortion: Theory and application

Qing Mao [a], Ulrike Krewer [a,b,*]

[a] *Max Planck Institute for Dynamics of Complex Technical Systems, Sandtorstr. 1, 39106 Magdeburg, Germany*
[b] *TU Braunschweig, Institute of Energy and Process Systems Engineering, Franz-Liszt-Str. 35, 38106 Braunschweig, Germany*

ARTICLE INFO

Keywords:
Methanol concentration
Methanol oxidation kinetics
Frequency response analysis
Nonlinear dynamic behavior

ABSTRACT

The nonlinear frequency response of a direct methanol fuel cell (DMFC) is studied by analyzing the total harmonic distortion (THD) spectra. The dependence of the THD spectra on methanol concentration and methanol oxidation kinetics is investigated by means of both simulation and experiment. Simulation using a continuous stirred tank reactor network model suggests that the methanol concentration profile in the anode has a strong impact on the THD spectra. The experimentally observed nonlinear behavior of the DMFC anode can be qualitatively reproduced with a model containing a three-step methanol oxidation mechanism with Kauranen–Frumkin/Temkin kinetics. Both experiment and simulation results show that THD value has a monotonic correlation with methanol concentration at certain frequencies and its sensitivity to concentration is improved with increased current amplitude. The monotonic relationship enables the THD to sense the methanol concentration level by the DMFC itself, which is of mayor interest for the portable application as an external sensor for the system can be omitted.

1. Introduction

Direct methanol fuel cell (DMFC) has drawn much attention as a promising power source due to high energy density and environmental friendliness. In recent years, although much progress has been achieved on its research [1–3], some issues still remain to be solved before it becomes a competitive technology, one of which is fuel cell online diagnosis. Electrochemical impedance spectroscopy (EIS) is a powerful tool to get online information of hydrogen fuelled proton exchange membrane fuel cell (PEMFC). It is usually used to diagnose membrane drying, cathode flooding and CO poising [4,5]. However, it fails to sense methanol concentration for the DMFC [6,7].

Conventional DMFCs suffer from a problem of methanol crossover. This diffusion-based flux of methanol from the anode to the cathode through the membrane electrolyte not only lowers fuel utilization efficiency but also adversely affects the oxygen cathode resulting in poorer cell performance. Methanol dosing therefore needs not only take into account consumption proportional to the applied current, but also to the – usually unknown – concentration of the feed entering the fuel cell [9]. In order to minimize cross-over, the concentration of methanol in the fuel feed stream is kept low (e.g., below 1 mol L^{-1}) by dilution with water. However, from the point of view of DMFC system, carrying pure methanol or high concentration methanol is necessary to achieve high volumetric energy density. To solve above contradictory concerns of the methanol concentration, the exhaust methanol solution and generated water needs to be recirculated back to the system with controlled addition of pure methanol [8]. Online concentration sensing provides feedback for the control of pure methanol injection into the anode feed and – as concentration is a function of crossover, current and injected fuel, offers indirect information of methanol crossover flux. Both of them allow DMFCs to keep a predetermined power output. Although sensor less control has been developed for DMFC static operation [9], methanol concentration information is still highly beneficial for DMFC systems when operated dynamically.

Fuel cells are nonlinear systems as they couple complex electrochemical processes with mass transport processes [10]. Especially, the electrochemical oxidation processes of C-containing fuels are known to have complex and highly nonlinear dynamic behaviour ranging from spontaneous oscillation to overshooting [11]. Krewer et al. [11] reviews the usage of dynamic methods on kinetics investigation, fuel concentration detection and performance improvement of fuel cells. Methods such as nonlinear frequency response analysis and current step analysis have shown some

Abbreviations: CSTR, continuously stirred tank reactor; DMFC, direct methanol fuel cell; THD, total harmonic distortion; EIS, electrochemical impedance spectroscopy.

* Corresponding author at: TU Braunschweig, Institute of Energy and Process Systems Engineering, Franz-Liszt-Str. 35, 38106 Braunschweig, Germany.
Tel.: +49 (0)531 391 3030; fax: +49 (0)531 391 5932.
E-mail address: u.krewer@tu-bs.de (U. Krewer).

promising results on fuel concentration sensing. As such, the authors highlight the necessity of more detailed research.

There is a wide variety of signals, ranging from single and multiple sinusoidal input signals to step-wise changes which enable to deflect an electrochemical system from its steady state and as such analyse its dynamic linear or nonlinear behaviour. This contribution focusses on the response to single sinusoidal excitations of large amplitudes. Fig. 1 shows a schematic diagram of the typical voltage response of a DMFC to an input current of sinusoidal form. The voltage response is displayed in both time domain and frequency domain. Besides a response at the excitation frequency, the voltage response contains additional contributions which are attributed to certain physico-chemical processes in the DMFC. Therefore, besides the response at the fundamental frequency of the input current, contributions at higher harmonic frequencies are also observed in the frequency domain of the voltage response. Those harmonic frequencies are a component frequency that is an integer multiple of the fundamental, or first harmonic, frequency. The voltage response at the fundamental frequency represents the linear response behaviour of the target system to the given sinusoidal deflection; however, the response observed at higher harmonic frequencies describes its nonlinear response behaviour. EIS employs the linear response information alone, which would inevitably conceal much detail in the analysis of the fuel cell systems [7,12]. Therefore, extracting nonlinear response information to sinusoidal input signals has been recognized as an effective way to extend the diagnosis scope for fuel cells.

Total harmonic distortion (THD) spectroscopy is widely used in audio system measurements. It can be used to characterize the nonlinear response behavior of a system as it contains the summed contribution of all higher harmonic frequencies. Ramschak et al. [13,14] propose that THD signals can be used as a state of the art monitor for PEMFC. From the point of view of applications, the advantage of using THD analysis is the low cost and the small size of the detection devices. Besides THD spectroscopy, higher order harmonic spectra can also be used to evaluate the nonlinear response behaviour. Wilson et al. [15,16] introduce nonlinear EIS (NLEIS) to describe the O_2 reduction processes in a solid oxide fuel cell (SOFC). From the difference of the third-order harmonic spectra, O_2 reduction on a perovskite oxide is suggested to be limited by O_2 dissociative adsorption. Kadyk et al. [12,17] compared the suitability of EIS and higher harmonic response for sensing the state of a PEMFC. According to their report, EIS changes similarly when the cell is CO-poisoned or in a dehydrated condition; as such, it cannot be used as a distinguish method. However, the second order (2nd) frequency response function (FRF) proved to be an effective way to make such a distinction. Recently, Bensmann et al. [18] conducted a model-based analysis of the effect of methanol oxidation reaction kinetics on the 2nd FRF. It is suggested that the changes observed in the 2nd FRF makes the nonlinear frequency response analysis as a suitable tool to discriminate among those assumed methanol reaction mechanisms. In summary, the nonlinear response of fuel cells to a sinusoidal input may generally be interesting for kinetic studies and state diagnosis of fuel cells. However, up to now, little work has been done on both theoretical understanding and experimental validation for the nonlinear frequency response of a DMFC [7].

We recently suggested that THD signals of a DMFC anode may be used to determine methanol concentration whereas the EIS is not feasible [7]. In this paper, the theoretical background to the THD detection, a systematic analysis of the correlation between THD and concentration as well as the key influential factors arising from fuel cell operation will be presented. Details of the THD simulation for a DMFC anode will be also given. The effect of methanol concentration, current amplitude and DMFC operation mode on the THD spectroscopy will be discussed using theoretical analysis and experimental validation.

2. Simulation

2.1. Dynamic model of a DMFC anode

One approach to better understand the nature of complex nonlinear response behavior of the DMFC is via THD simulation. The THD simulation for a DMFC anode can be realized using its dynamic modeling equations. As depicted in Fig. 2, the anode compartment is composed of anode channel and anode reaction region (i.e. gas diffusion electrode). The anode channel is assumed to be a network of continuous stirred tank reactor (CSTR) modules in series, which could effectively reproduce the methanol concentration variation along the single serpentine channel used in the experiment [19]. Each mentioned CSTR is also additionally connected to a CSTR that represents the attached anode reaction region. The CSTR module of the anode channel and the attached one of the reaction region constitute a CSTR segment.

The volume of each CSTR in the anode compartment is calculated as follows:

$$V^{i,CSTR} = \frac{V^i}{n} \quad i = A, AR \tag{1}$$

where the superscript A and AR represent the anode channel and the anode reaction region, respectively. V is the volume and n is the number of CSTR modules of either anode channel or anode reaction region. Similarly, the geometric electrode area of each CSTR

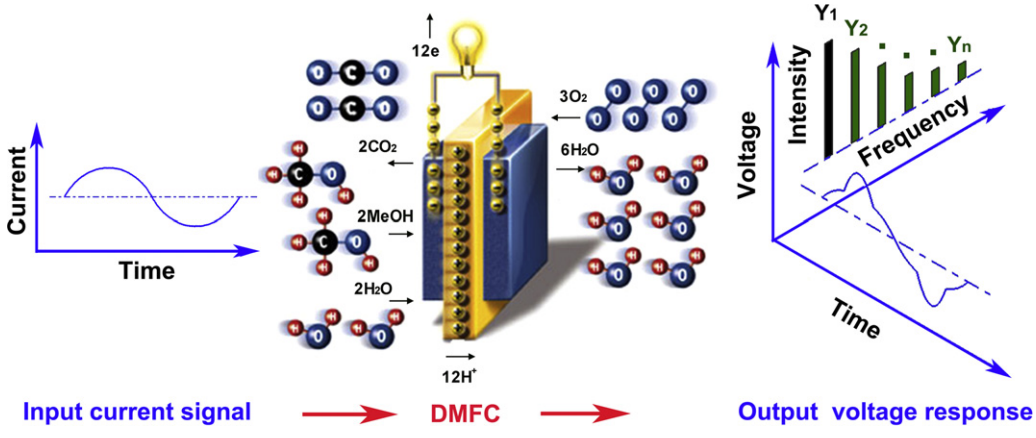

Fig. 1. Schematic diagram for the voltage response of a DMFC to a sinusoidal input of current in both time domain and frequency domain.

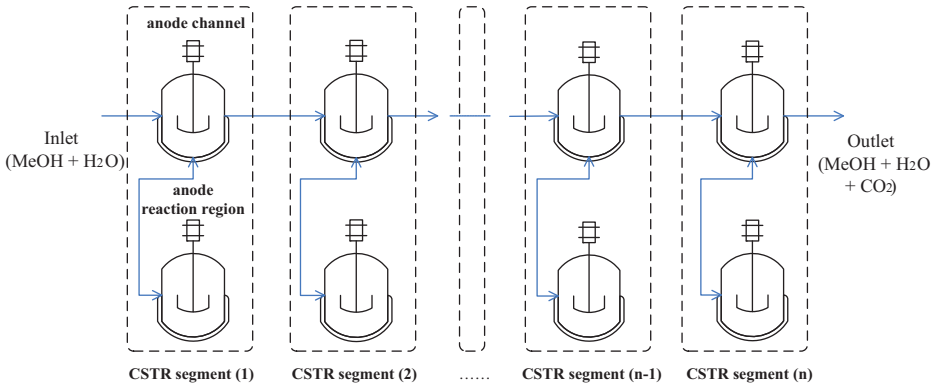

Fig. 2. CSTR network model for a DMFC anode with a single serpentine channel.

segment is calculated by taking into account the whole area of the anode (A_s) and the number of CSTRs, which is shown in Eq. (2).

$$A_s^{CSTR} = \frac{A_s}{n} \tag{2}$$

In the anode reaction region, comparative studies are performed by employing two different methanol oxidation kinetic models to investigate the influence arising from the intermediates. One is a methanol one-step reaction mechanism based on Butler–Volmer equation [20]. The other is a methanol three-step oxidation mechanism with Kauranen–Frumkin/Temkin kinetics [21,22]. The enrolled reaction steps as well as the model equations in both anode channel and anode reaction region are listed in Table 1. A detailed variable and parameter declaration is given in the nomenclature. The parameters of the methanol oxidation kinetics are taken from the respective literature [20,22].

In the dynamic model, anode potential U_a (vs. DHE) of the DMFC is identical for all CSTR segments, which is assumed to be the anode overpotential $\{\eta_a\}$. However, the anode current of all CSTR modules is summed to yield the total cell current:

$$A_s i_{cell} = \sum_k A_{cell}^{CSTR} i_{cell}^k \tag{3}$$

where i_{cell} and i_{cell}^k are the current density of the total electrode and that of CSTR segment k, respectively.

2.2. THD simulations for DMFC anode

Anode THD simulation is achieved by applying a sinusoidal current to the dynamic model. The excitation current is illustrated as:

$$j(t) = j_{dc} + j_{ac} \cdot \sin(\omega \cdot t) \tag{4}$$

The anode voltage response of the model is then received in the time domain. After expanding the time domain voltage response into a Fourier series in form as Eq. (5), the voltage response at the fundamental frequency and that at higher harmonic frequencies are obtained.

$$U_a(t) = U_{a,dc} + \sum_{k=1}^{\infty} (U_{ac,k}\varphi_k(t) + U_{as,k}\psi_k(t)) \tag{5}$$

where φ_k and ψ_k are normalized basis functions, which are shown in Eqs. (6) and (7), respectively. The subscript k is the order of the Fourier approximation.

$$\varphi_k(t) = \sqrt{\frac{\omega}{\pi}} \cos(k\omega t) \tag{6}$$

$$_k(t) = \sqrt{\frac{\omega}{\pi}} \sin(k\omega t) \tag{7}$$

$U_{a,dc}$ is the mean value of anode potential. The coefficients $U_{ac,k}$ (of the cos-terms) and $U_{as,k}$ (of the sin-terms) are given by the following integrals:

$$U_{ac,k} = \int_0^T U_a(t) \cdot \varphi_k(t) dt \tag{8}$$

$$U_{as,k} = \int_0^T U_a(t) \cdot \psi_k(t) dt \tag{9}$$

Therefore, the Fourier series can be rewritten as:

$$U_a(t) = U_{a,dc} + \sum_{k=1}^{\infty} U_{total,ak}\varphi_k(t + \tilde{\vartheta}_k) = U_{a,dc} + \sum_{k=1}^{\infty} U_{total,ak} \sqrt{\frac{\omega}{\pi}} \cos(k\omega t + \vartheta_k) \tag{10}$$

with

$$U_{total,ak} = \sqrt{U_{ac,k}^2 + U_{as,k}^2} \tag{11}$$

where $U_{total,ak}$ is the root mean square (RMS) amplitude of the anode voltage at angular frequency $k\omega$ and ϑ_k is the phase shift.

Analogous to the THD definition in audio systems [23], the THD of fuel cell systems can be defined as the ratio of the sum of the amplitude of the voltage response of all higher harmonic frequencies ($k \geq 2$) to that of the fundamental frequency ($k = 1$):

$$\mathrm{THD} = \frac{\sqrt{\sum_{k=2}^{\infty} U_{total,ak}^2}}{U_{total,a1}} \tag{13}$$

In this article, the simulated voltage amplitudes ranging from the fundamental frequency to the 10th harmonic frequency are used to calculate THD. All simulation was performed using a commercial software package (MATLAB R2010b, the MathWorks Inc.). The relative error tolerance for the initial value problem of ordinary differential equations is 10^{-12}.

3. Experimental

A commercial membrane electrode assembly (MEA, type M241) for DMFC application from Johnson Matthey Co. is used for all measurements. PtRu/C with platinum loading of 2.7 mg cm^{-2} and ruthenium loading of 1.35 mg cm^{-2} is used as the catalyst for the anode. Pt/C with platinum loading of 2.0 mg cm^{-2} is used as the catalyst for the cathode. Nafion®-115 membrane is the electrolyte. The active area of MEA is 26 cm^2. A single cell was completed by sandwiching the MEA between two carbon plates containing one

Table 1
Model equations of the DMFC anode.

Anode channel	$\frac{dc^{A,i}_{CH_3OH}}{dt} = \frac{F^{A,i}}{V^{A.CSTR}}\left(c^{A,i-1}_{CH_3OH} - c^{A,i}_{CH_3OH}\right) - \frac{D_{CH_3OH}\cdot\varepsilon^{1.5}\cdot A^{CSTR}_S}{d^{AR}\cdot V^{A.CSTR}}\left(c^{A,i}_{CH_3OH} - c^{AR,i}_{CH_3OH}\right), \quad i = 1\cdots n$	(T1.1)
	$dc^{AR,i}_{CH_3OH} = \frac{D_{CH_3OH}\cdot\varepsilon^{1.5}\cdot A^{CSTR}_S}{d^{AR}\cdot V^{AR.CSTR}}\left(c^{A,i}_{CH_3OH} - c^{AR,i}_{CH_3OH}\right) - \frac{A^{CSTR}_S}{V^{AR.CSTR}}R^i_{A1}, \quad i = 1\cdots n$	(T1.2)
	One-step reaction	
	$CH_3OH + H_2O \xrightarrow{R_{A1}} CO_2 + 6H^+ + 6e^-$	(T1.3)
Anode reaction region	$\frac{d\eta^i_A}{dt} = \frac{1}{C^{AR}\cdot c^i_{cell}} - \frac{1}{C^{AR}}6FR^i_{A1}$	(T1.4)
	$R^i_{A1} = \frac{c^{AR,i}_{MeOH}}{c^{AR,i}_{MeOH} + c^{lim}_{MeOH}}\frac{ai_0}{6F}\exp\left(\frac{\alpha_a F}{RT}\eta^i_A\right) - \exp\left(-\frac{\alpha_c F}{RT}\eta^i_A\right)$	(T1.5)
	Three-step reaction	
	(Pt) $CH_3OH \xrightarrow{R_{A1}} CH_3OH_{ads} \rightarrow \cdots \xrightarrow{-3H^+-3e^-} CO_{ads} + H^+ + e^-$	(T1.6)
	(Ru) $H_2O \xrightarrow[R_{A2}/R_{A-2}]{} {}^*OH_{ads} + H^+ + e^-$	(T1.7)
	(Pt/Ru) $CO_{ads} + OH_{ads} \xrightarrow{R_{A3}} CO_2 + H^+ + e^-$	(T1.8)
	$\frac{d\theta^i_{CO}}{dt} = \frac{1}{c_{Pt}}\left(R^i_{A1} - R^i_{A3}\right)$	(T1.9)
	$\frac{d\theta^i_{OH}}{dt} = \frac{1}{c_{Ru}}\left(R^i_{A2} - R^i_{A3}\right)$	(T1.10)
	$\frac{d\eta^i_A}{dt} = \frac{1}{C^{AR}\cdot c^i_{cell}}i^i_{cell} - \frac{1}{C^{AR}}FR^i_A$	(T1.11)
	$R^i_A = 4R^i_{A1} + R^i_{A2} + R^i_{A3}$	(T1.12)
	$R^i_{A1} = R_{A10}\cdot\exp\left(-\beta_{CO}\cdot g_{CO}\cdot\left(\theta^i_{CO} - 0.5\right)\right)\cdot c^{AR,i}_{CH_3OH}\cdot\left(1-\theta^i_{CO}\right)$	(T1.13)
	$R^i_{A2} = R_{A20}\cdot\exp\left(\frac{\alpha_A F}{RT}\eta^i_A\right)\exp\left(-\beta_{OH}\cdot g_{OH}\cdot\left(\theta^i_{OH} - 0.5\right)\right)\cdot c^{AR,i}_{CH_3OH}\cdot\left(1-\theta^i_{OH}\right) - R_{A-20}\cdot\exp\left(-\frac{(1-\alpha_A)F}{RT}\eta^i_A\right)\exp\left((1-\beta_{OH})\cdot g_{OH}\cdot\left(\theta^i_{OH} - 0.5\right)\right)\cdot\theta^i_{OH}$	(T1.14)
	$R^i_{A3} = R_{A30}\cdot\exp\left(-\beta_{CO}\cdot g_{CO}\cdot\left(\theta^i_{CO} - 0.5\right)\right)\cdot\theta^i_{CO}\cdot\theta^i_{OH}$	(T1.15)

Fig. 3. Effect of series-connected CSTR segment number on simulated anode THD.

single serpentine channel each, gold-plated copper current collectors and stainless steel end plates. A torque of 8 N m was exerted on the screws, which hold together the steel back plates.

To record the THD of the anode alone, the DMFC was operated in half cell mode. In this mode, the anode was supplied with aqueous methanol with a flow rate of 5 mL min^{-1} and served as the working electrode. The employed methanol concentrations range from 0.3 mol L^{-1} to 1.0 mol L^{-1}. The cathode was fed with humidified H_2 at 60 °C with a flow rate of 250SCCM and acted as counter electrode and dynamic hydrogen reference electrode (DHE). The cell temperature is 60 °C. THD spectroscopy of the DMFC was measured by Zahner impedance measurement units (Zennium and PP241) over a frequency range from 1×10^3 Hz to 0.01 Hz. The DC offset is 2.5 A and the current amplitude is 0.5 A, corresponding to 0.096 A cm^{-2} and 0.019 A cm^{-2}, respectively. The voltage amplitude from the first harmonic frequency to the 10th harmonic frequency is recorded to determine the THD. To obtain the error bar of the THD spectra, each measurement was reproduced for three times. In addition, similar THD measurements were also performed for the DMFC in fuel cell mode, in which dry air with a flow rate of 500SCCM was fed to the cathode.

4. Results and discussion

4.1. Effect of CSTR module number on THD simulations of DMFC anode

As mentioned in Section 2.1, the anode channel is simulated as CSTR modules in series. The total number of CSTRs determines the concentration profile in the anode. In order to examine the influence of the concentration profile on the nonlinear response behavior of the DMFC anode, THD simulation is performed for the same anode with different total number of the CSTR segments. Fig. 3 shows the simulated anode THD spectra at the DC offset of 0.096 A cm^{-2}. The methanol three-step oxidation mechanism with Kauranen–Frumkin/Temkin kinetics is employed in the anode dynamic model. It can be observed that THD value decreases with increased total number of CSTR segments in the frequency range below 0.015 Hz. In the frequency range from 0.015 Hz to 20 Hz, THD magnitude increases with increased number of segments. Finally, in the frequency higher than 20 Hz, the THD peak, which is only for models with a few CSTRs, reduces to a negligible level with increased total number of CSTR segments. It is also obvious that

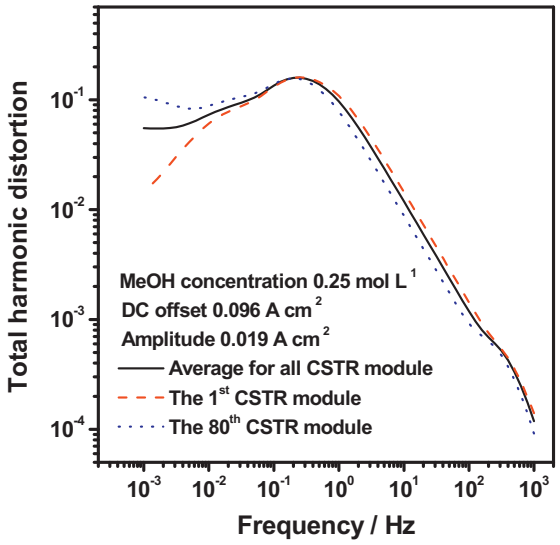

Fig. 4. Simulated THD of the first and the final CSTR segment as well as the THD contributed from all CSTR segments for a model with 80 series-connected CSTR segments.

the THD value in the whole frequency range changes little when the total number of CSTR segments changes from 60 to 100.

Fig. 4 shows the local THD spectra of the first CSTR segment and the final one when the anode employs 80 CSTR segments. The anode THD as a whole is also shown in the figure. The inlet methanol concentrations were 0.25 mol L^{-1} and 0.19 mol L^{-1} for the first and the final CSTR module of the anode channel, respectively. It can be observed that the THD contributed by all CSTR segments falls in between the THD of the first CSTR segment and that of the final one.

Above simulations indicate that the anode THD represents the gross nonlinear behavior from all employed CSTR segments and confirm that the total number of CSTRs determines not only the concentration profile, but also the THD profile in the anode. Therefore, the number of CSTR segments should be selected as high as possible to illustrate a realistic methanol concentration distribution along the experimental single serpentine channel. Similar conclusions can also be found in the local EIS simulation for the PEMFC cathode [24]. Here, considering the THD variation with CSTR segment number as show in Fig. 3 and the program execution time (1.24×10^4 s for 80 CSTR segments), 80 CSTR segments are considered as a suitable selection for anode THD simulation.

4.2. Effect of methanol concentration and methanol oxidation kinetics on the simulated THD of DMFC anode

With above determined dynamic CSTR network model, the simulated anode THD spectra with different input methanol concentrations are given in Fig. 5(a) and (b) for the one-step and the three-step kinetics, respectively. In the frequency range less than 6.3×10^{-3} Hz, THD decreases first and then increases with decreased methanol concentration for both methanol oxidation kinetics. However, in the high frequency region, THD change is different for methanol oxidation mechanisms. As shown in Fig. 5(a), THD of the anode employing the methanol one-step oxidation mechanism decreases first and then increases with decreased methanol concentration in the frequency ranging from 6.3×10^{-3} Hz to 0.1 Hz. However, for the frequencies above 0.1 Hz, the THD is insensitive to methanol concentration. The THD is constant at a frequency range from 0.1 Hz to 6.3 Hz; it decreases with further increased frequency. Fig. 5(b) shows the THD spectroscopy of the anode that employs the methanol three-step reaction

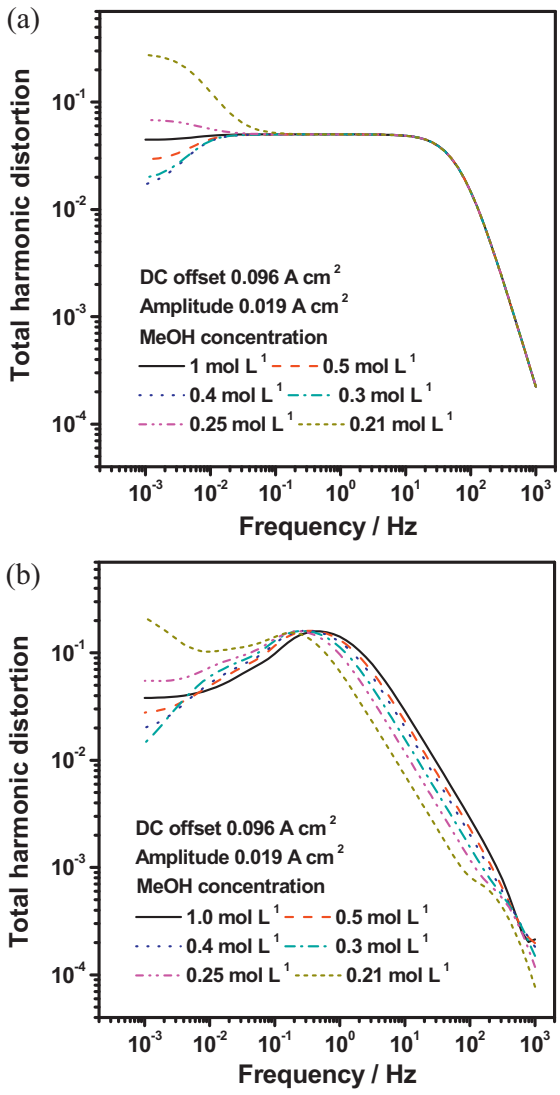

Fig. 5. Simulated THD spectra of the DMFC anode with different methanol concentrations and different methanol oxidation mechanisms: (a) methanol one-step oxidation mechanism and (b) methanol three-step oxidation mechanism with Kauranen–Frumkin/Temkin kinetics.

mechanism with Kauranen–Frumkin/Temkin kinetics. A maximum of THD can be observed in the frequency range from 6.3×10^{-3} Hz to 63 Hz. The maximum shifts to the high frequency range with increasing methanol concentration. As a result, a monotonous correlation between THD value and methanol concentration can be found in two frequency regions: THD decreases with increasing methanol concentration in the frequency domain range from 6.3×10^{-3} Hz to 0.125 Hz and increases in the frequency range from 0.5 Hz to 63 Hz.

As noted above, methanol transfer and its electrochemical oxidation take place in each CSTR segment. For a certain CSTR network, the inlet methanol concentration defines both the concentration profile and the THD profile in the anode. The latter contribute to the anode THD as a whole. During the simulation processes, Fick's law with a constant diffusion coefficient is used to describe methanol transport processes. It is a typical linear process which contributes nothing to the anode THD. Electrochemical reaction kinetics is therefore the only source for the nonlinear response of the DMFC anode. As such, the monotonous dependence of the THD of the complex kinetics on concentration in the high frequency domain (6.3×10^{-3} Hz to 63 Hz) should be attributed to the

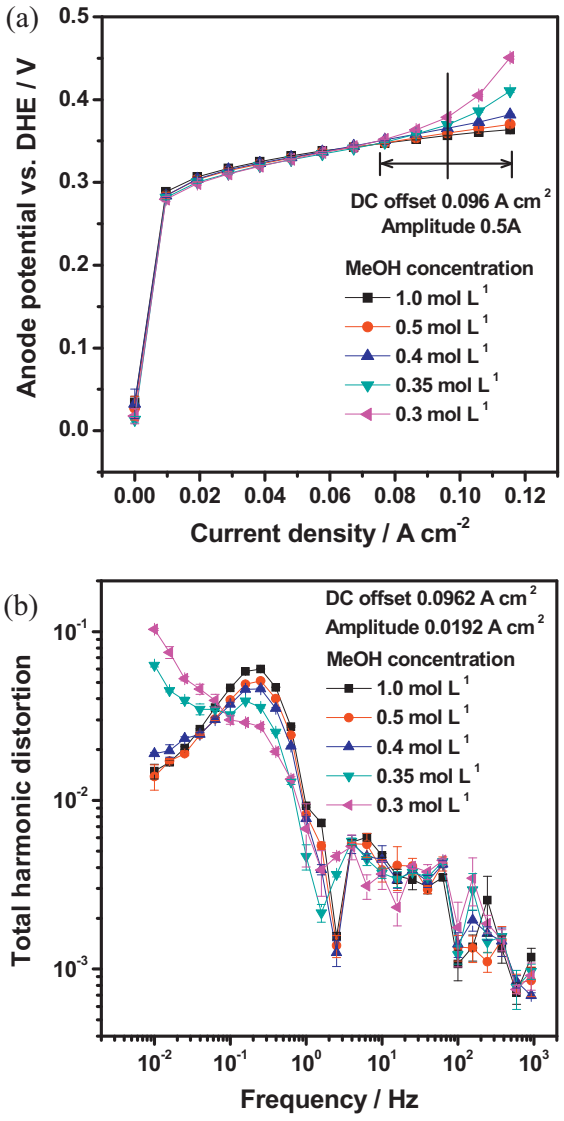

Fig. 6. Experimental IR corrected anode performance and THD spectra of the DMFC in half cell mode for different methanol concentrations: (a) IR corrected anode performance and (b) THD spectra at the DC offset of 0.096 A cm^{-2}.

formation and oxidation of the intermediates CO_{ads} and OH_{ads} in the methanol electro-oxidation processes. From another perspective, the methanol one-step reaction mechanism, which contains no adsorbed species, is also found to have a much smaller dynamic behavior to a step change in current than a multi-step mechanism [25], such as the three-step mechanism employing the intermediates OH and CO. Such a difference also indicates the possible difference existing in the nonlinear dynamic response for different methanol oxidation kinetics, since the voltage overshooting to a step change in current contains both linear and nonlinear response information [19].

4.3. THD experimental validation for DMFC anode

In order to determine which kinetics employed in above section is closer to reality, experiment validation of the anode THD is performed in this section. Fig. 6(a) shows the experimentally recorded IR corrected anode polarization curve with different methanol concentrations for a DMFC operated in half cell mode. It can be seen that anode overpotential decreases with increased methanol concentration in the high current density region, (0.077–0.115 A cm^{-2}). At the DC offset of 0.096 A cm^{-2}, THD measurement is performed using an amplitude of 0.019 A cm^{-2}. As shown in Fig. 6(b), the experimental THD changes significantly with methanol concentrations in the frequency range less than 10 Hz. With increased methanol concentration, THD increases in the frequency range from 0.1 Hz to 0.63 Hz. Below 0.04 Hz, THD decreases with increased methanol concentration for low methanol concentrations and becomes insensitive to concentration above 0.4 mol L^{-1}.

When DMFC is operated in half cell mode, H_2 evolution takes place in the counter electrode. It is a fast process due to the high exchange current density of hydrogen evolution on platinum surface. Although two-step mechanisms (i.e. Volmer–Tafel and Volmer–Heyrovsky) are found more suitable for the H_2 evolution process [26,27], in house experimental THD spectra of the H_2/H_2 cell show that such a relationship with respect to the input current and the voltage response contributes little to the THD signals in the sensitive frequency domain for methanol concentration. In addition, as the Nafion® membrane is well humidified, the proton conduction in the electrolyte that obeys ohmic law can also be taken as a linear process. Therefore, THD spectroscopy of the DMFC in half cell mode can be taken as being influenced solely by the anode.

The comparison between the experimental and simulated THD spectra shows that the THD model adopting the three-step methanol oxidation mechanism with Kauranen–Frumkin/Temkin kinetics is much closer to experiment than the one with a one-step mechanism, as both experiment and model with three-step mechanism show the maximum THD between 0.1 Hz and 1 Hz and the THD dependence on methanol concentration in either side of the maximum. The monotonous correlation between experimental THD and methanol concentration can be seen in the THD simulation with the three-step mechanism, but not in that with the one-step mechanism. According to the knowledge gained by simulation (Section 4.2), the experimental THD response in the frequency range from 0.1 Hz to 0.63 Hz and that in the frequency range from 0.01 Hz to 0.04 Hz should be attributed to the change in nonlinear dynamics caused by formation and oxidation of the intermediates in the methanol electro-oxidation processes. The observed sensitivity at 0.1–0.63 Hz closely agrees with the sensitivity to the voltage response (0.1–5 s) after a step change in current [11], which could also be deduced to the same oxidation kinetics. In contrast to the impedance results [7], such a monotonous relationship obtained between THD value and methanol concentration at certain frequency region may be exploited for sensing methanol concentration level for a DMFC in half cell mode.

4.4. Effect of current amplitude on nonlinear response behavior of DMFC anode

According to the THD definition as shown in Eq. (13), THD contains both linear and nonlinear frequency response information. The linear response, i.e. voltage response at the fundamental frequency, can be calculated by the product of input current and magnitude of the EIS, as shown in Eq. (14).

$$U_{total,a1} = |Z| \cdot j_{ac} \tag{14}$$

Since the amplitude of the input current is constant, the EIS can reflect the denominator variation of the defined THD. Fig. 7 shows the experimental EIS of the DMFC in half cell mode with different amplitude in Bode diagram. It can be observed that the magnitude of the EIS changes little with amplitude in the whole frequency domain.

The norm of the voltage response for all higher harmonic frequencies $\left(\sqrt{\sum_{k=2}^{\infty} U_{total,ak}^2}\right.$ is the contribution of the nonlinear

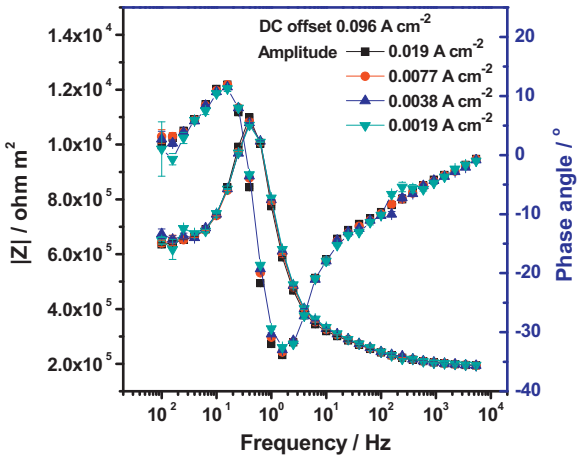

Fig. 7. Experimental EIS with different current amplitudes for the DMFC in half cell mode.

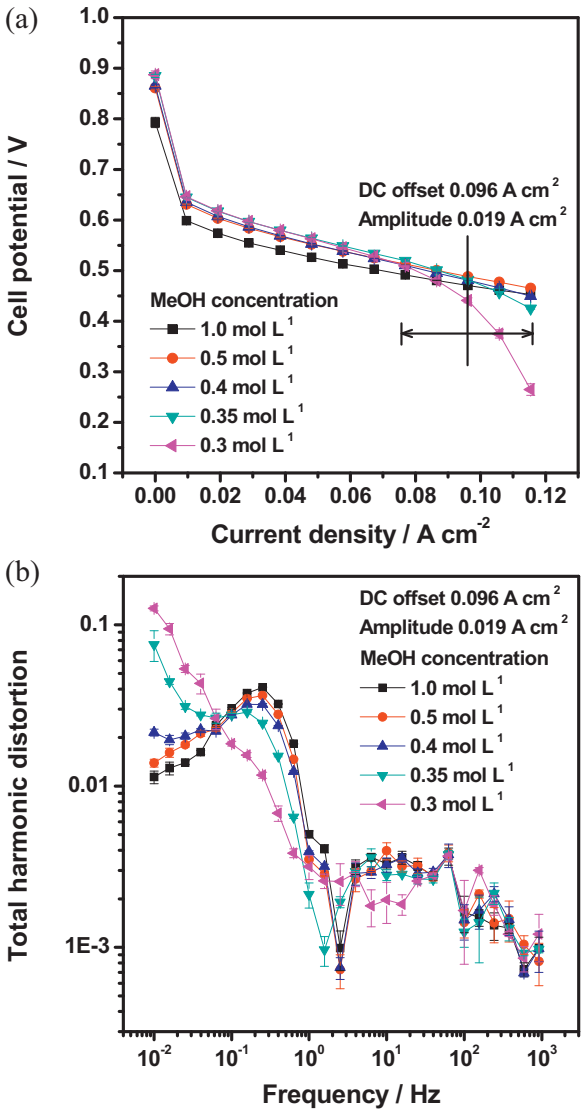

Fig. 9. Cell performance and THD spectra of the DMFC in fuel cell mode for different methanol concentrations: (a) cell performance and (b) THD spectra at the DC offset of 0.096 A cm^{-2}.

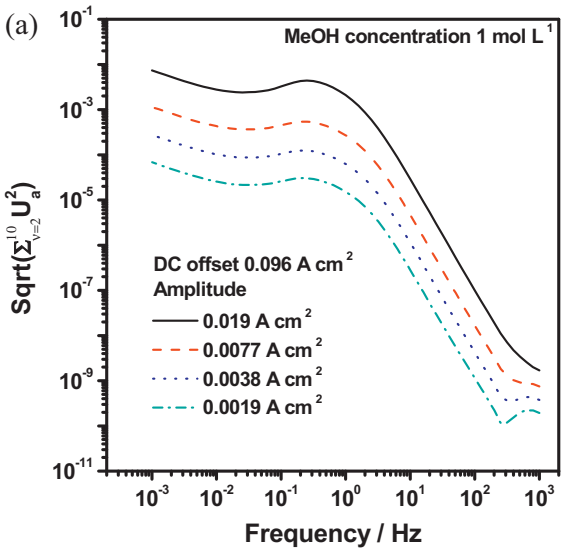

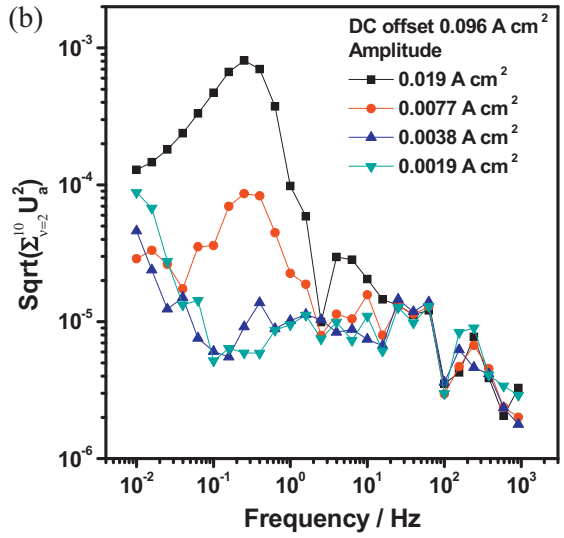

Fig. 8. Comparison between simulated nonlinear term of the THD spectra and experimental one for the DMFC in half cell mode with different current amplitudes: (a) simulation and (b) experiment.

dynamics of the DMFC anode, which is the numerator of the defined THD. Fig. 8(a) shows its simulation results with current amplitudes when the model adopts the methanol three-step oxidation mechanism with Kauranen–Frumkin/Temkin kinetics. The norm of the nonlinear response increases with increased amplitude in the whole frequency domain. However, as shown in Fig. 8(b), the experimental norm displays a different tendency. When the current amplitude increases from 0.0038 A cm^{-2} to 0.019 A cm^{-2}, THD increases in the frequency range from 0.01 to 10 Hz; it changes little for the frequencies above 10 Hz. For very small values of 0.0019 A cm^{-2} to 0.0038 A cm^{-2}, the norm is not influenced by the amplitude. With such small amplitudes, resolution of the device and external noise may have a dominating influence on the norm.

As is known, system error arising from the measuring instruments is inevitable in electrochemical experiments. THD spectra with methanol concentrations can be presented only when both linear and nonlinear part of the voltage response are higher than the voltage resolution of respective measurement module or the external noise. Above EIS variation with amplitudes indicates the amplitude of 0.0019 A cm^{-2} is high enough to get linear part of the voltage response in the whole frequency domain. However, the

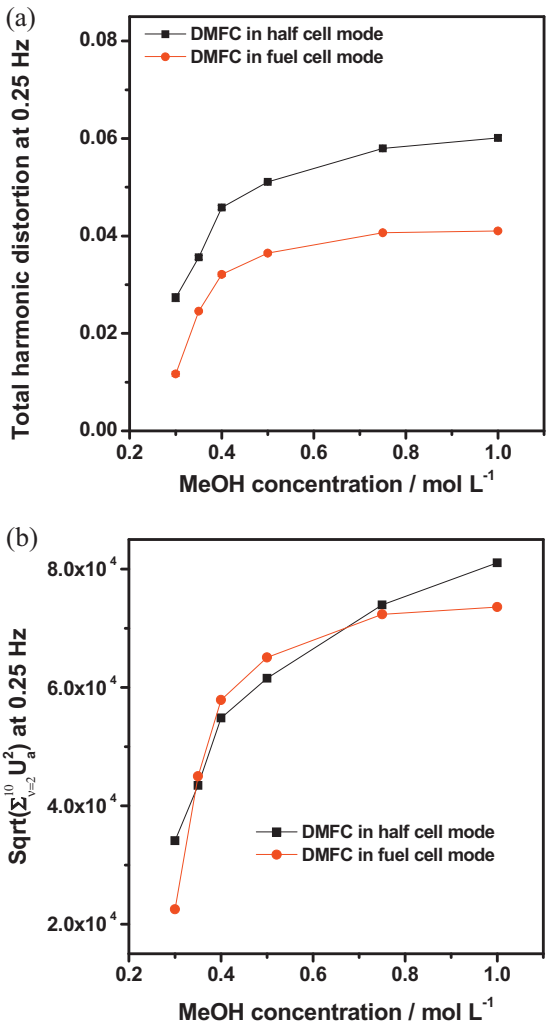

Fig. 10. THD spectra as well as the corresponding norm of the nonlinear contribution of the DMFC in both half cell mode and fuel cell mode for different methanol concentrations at the frequency of 0.25 Hz: (a) THD and (b) norm of the nonlinear response.

results in Fig. 8(b) suggest that the nonlinear part of the voltage response is not reflected in the measured THD in the whole frequency range when the amplitude is lower than 0.0038 A cm^{-2}. This may be attributed to the fact that the voltage intensity at higher harmonic frequencies reduces to a level less than the resolution of the measurement or system noise. In the frequency range less than 10 Hz, the experimentally observed change of the norm form 0.0077 A cm^{-2} to 0.0192 A cm^{-2} is same as the simulations (Fig. 8(a)); as such the amplitude of 0.0192 A cm^{-2} is high enough to get nonlinear response information of the anode. Simulations involving insufficient resolution of harmonic detection module can reproduce the experimental observed behavior of THD spectra.

4.5. THD spectra of the DMFC in fuel cell mode

From above, it is suggested that THD analysis could be used to sense methanol concentration quantitatively when the DMFC operates in half cell mode. In order to check whether the method may be implemented online in DMFC systems, THD spectra are also recorded for a DMFC operated in fuel cell mode. Fig. 9(a) shows the polarization curve of the DMFC with different inlet methanol concentrations. The cathode is fed with air at a flow rate equivalent to an O_2 excess ratio of 9.8. In the low current density region (less than 0.04 A cm^{-2}), the cell voltage decreases with increased methanol concentration, which can be attributed to increased methanol crossover. In the high current density region (higher than 0.08 A cm^{-2}), mass transport voltage loss decreases with increased inlet methanol concentration.

Fig. 9(b) shows the experimental THD spectra recorded at 0.096 A cm^{-2} with different methanol concentrations. With increased methanol concentration, THD increases in the frequency region range from 0.1 Hz to 0.63 Hz and decreases in the frequency domain from 0.01 Hz to 0.04 Hz. The THD spectra in fuel cell mode show the same feature and dependence on concentration in a given frequency range compared with the spectra in half cell mode (Fig. 6(b)). Therefore, methanol concentration detection can be also correlated with THD at certain frequencies for the DMFC in fuel cell mode.

Fig. 10(a) shows the THD results at 0.25 Hz with different methanol concentrations at the DC offset of 0.096 A cm^{-2} for the DMFC in both half cell mode and fuel cell mode. THD shows a monotonous increase with inlet methanol concentration in both operating modes. The THD value of the cell in half cell mode is higher than that in fuel cell mode. Fig. 10(b) also shows the nonlinear norm of the respective THD. It can be observed that the norm increases with increased methanol concentration in both operate modes. The nonlinear norm of the THD in half cell mode is close to that in fuel cell mode. When the methanol concentration is in range from 0.35 mol L^{-1} to 0.5 mol L^{-1}, the norm in half cell mode is slightly lower than that in fuel cell mode, however, a contrary tendency is observed for the concentration at 0.3 mol L^{-1} and that higher than 0.75 mol L^{-1}.

In fuel cell mode, O_2 reduction and the oxidation of the crossover methanol take place in the DMFC cathode simultaneously. These processes may contribute slightly to the nonlinear response of the DMFC and cause the observed difference between the nonlinear terms of the THD between fuel cell mode and half cell mode (Fig. 10(b)). In house experiments showed that O_2 stoichiometry could influence the nonlinear response behavior of PEMFC in the frequency range less than 15.8 Hz. More in-depth studies on the cathode THD of DMFC with regard to O_2 transfer and reduction processes as well as crossover methanol oxidation processes are still ongoing. However, for the here investigate case of high cathode stoichiometric feed, the difference of the absolute THD values at 0.25 Hz between the half cell mode and the fuel cell mode can be mostly attributed to the voltage response variation at the fundamental frequency. The nonlinear response behavior of the DMFC to a sinusoidal input current at 0.25 Hz is in this case mainly determined by the anode kinetics. As such, the correlation between THD of a DMFC and inlet concentration may be exploited for sensing the methanol concentration level in a DMFC – this holds at least in case the DMFC is operated at defined, high cathodic stoichiometry.

5. Conclusions

In the presented work, nonlinear frequency response of a DMFC has been studied using the concept of THD. THD simulation is performed for the DMFC anode by employing a dynamic CSTR network model. Subsequently, its experimental validation is completed for the DMFC in half cell mode. Simulation results show that increasing the series-connected CSTR segment number enable to model the methanol concentration profile and consequent THD profile along the single serpentine channel. Only the anode model adopting the methanol three-step oxidation mechanism with Kauranen–Frumkin/Temkin kinetics is able to reproduce basic features of the experimental THD spectra. THD shows a monotonous correlation with methanol inlet concentration in both half-cell mode and fuel cell mode at certain frequencies, which enable THD

analysis to sense methanol concentration during fuel cell operation and by using fuel cell itself as a sensor. However, to avoid disturbance from the system error, a current stimulus with high amplitude is confirmed to be necessary.

Acknowledgements

The authors acknowledge the support of this work by the Alexander von Humboldt Foundation and thank Dr.-Ing. Richard Hanke-Rauschenbach and Prof. Manfred Wilhelm for fruitful discussion in the field of nonlinear frequency response analysis.

Appendix A. Nomenclature

A_s geometric electrode area of the DMFC = 2.6×10^{-3} [m^2]
A_s^{CSTR} geometric electrode area of a CSTR segment [m^2]
c_{Pt} surface concentration of Pt = 0.011 [mol m^{-2}]
c_{Ru} surface concentration of Ru = 0.121 [mol m^{-2}]
$c_{CH_3OH}^{A,in}$ inlet methanol concentration [mol m^{-3}]
$c_{CH_3OH}^{A,i}$ methanol concentration inside the anode channel for segment i, [mol m^{-3}]
$c_{CH_3OH}^{AR,i}$ methanol concentration in the anode reaction region for segment i [mol m^{-3}]
C^{AR} anode double layer capacitance [F m^{-2}]
d_{AR} thickness of anode reaction region, 230×10^{-6} [m]
D_{CH_3OH} diffusion coefficient of methanol in water at 333 K = 3.187×10^{-9} [m^2 s^{-1}]
F Faraday constant = 96,485 [C mol^{-1}]
F^A flow rate of the methanol solution entering the anode = 8.333×10^{-8} [m^3 s^{-1}]
g_{CO} inhomogeneity/interaction factor for Frumkin/Temkin adsorption on Pt = 6.82
g_{OH} inhomogeneity/interaction factor for Frumkin/Temkin adsorption on Ru = 0.43
j_{cell} cell current density = 960 [A m^{-2}]
j_{cell}^i cell current density of CSTR segment i [A m^{-2}]
n numbers of CSTR segment = 80
r_{An}^i reaction rate for anode reaction step n in CSTR segment i
r_{A10} reaction rate constant for anode reaction step 1 = 1.6×10^{-4} [m s^{-1}]
r_{A20} reaction rate constant for anode reaction step 2 = 7.2×10^{-4} [mol m^{-2} s^{-1}]
r_{A-20} reaction rate constant for backward reaction of anode reaction step 2 = 9.91×10^4 [mol m^{-2} s^{-1}]
r_{A30} reaction rate constant for anode reaction step 3 = 0.19 [mol m^{-2} s^{-1}]
R universal gas constant = 8.314 [J mol^{-1} K^{-1}]
t time [s]
T cell temperature = 333.15 [K]
V^A volume of anode channel = 1.385×10^{-6} [m^3]
$V^{A,CSTR}$ volume of anode channel region in a CSTR module [m^3]
V^{AR} volume of anode reaction region 6.24×10^{-7} [m^3]
$V^{AR,CSTR}$ volume of anode reaction region in a CSTR module [m^3]
α_A charge transfer coefficient for anode reaction step 2 = 0.5
$\beta_{CO}(\beta_{OH})$ symmetry parameter for Frumkin/Temkin adsorption on Pt (Ru) = 0.5
ε porosity of anode reaction region, 0.885
η_A^i anode overpotential of module i [V]
θ_{CO}^i surface coverage of Pt with CO_{ads} in module i
θ_{OH}^i surface coverage of Ru with OH_{ads} in module i

Superscripts
A anode channel
A, in entering the anode compartment
AR anode reaction region
$CSTR$ CSTR module

References

[1] S. Gottesfeld, J. Power Sources 171 (2007) 37.
[2] Q. Mao, G.Q. Sun, S.L. Wang, H. Sun, G.X. Wang, Y. Gao, A.W. Ye, Y. Tian, Q. Xin, Electrochim. Acta 52 (2007) 6763.
[3] Q. Mao, G.Q. Sun, S.L. Wang, H. Sun, Y. Tian, J. Tian, Q. Xin, J. Power Sources 175 (2008) 826.
[4] J.M. Le Canut, R.M. Abouatallah, D.A. Harrington, J. Electrochem. Soc. 153 (2006) A857.
[5] N. Wagner, M. Schulze, Electrochim. Acta 48 (2003) 3899.
[6] P. Piela, R. Fields, P. Zelenay, J. Electrochem. Soc. 153 (2006) A1902.
[7] Q. Mao, U. Krewer, R. Hanke-Rauschenbach, Electrochem. Commun. 12 (2010) 1517.
[8] F. Zenith, C. Weinzierl, U. Krewer, Chem. Eng. Sci. 65 (2010) 4411.
[9] F. Zenith, U. Krewer, Energy Environ. Sci. 4 (2011) 519.
[10] C.B. Boyadjiev, V.N. Babak, Nonlinear Mass Transfer and Hydrodynamic Stability, 1st edition, Elsevier, Amsterdam, 2000.
[11] U. Krewer, T. Vidakovic-Koch, L. Rihko-Struckmann, ChemPhysChem 12 (2011) 2518.
[12] T. Kadyk, R. Hanke-Rauschenbach, K. Sundmacher, J. Electroanal. Chem. 630 (2009) 19.
[13] E. Ramschak, V. Peinecke, P. Prenninger, T. Schaffer, W. Baumgartner, V. Hacker, Fuel Cells Bull. 10 (2006) 12.
[14] E. Ramschak, V. Peinecke, P. Prenninger, T. Schaffer, V. Hacker, J. Power Sources 157 (2006) 837.
[15] J.R. Wilson, D.T. Schwartz, S.B. Adler, Electrochim. Acta 51 (2006) 1389.
[16] J.R. Wilson, M. Sase, T. Kawada, S.B. Adler, Electrochem. Solid-State Lett. 10 (2007) B81.
[17] T. Kadyk, R. Hanke-Rauschenbach, K. Sundmacher, J. Appl. Electrochem. 41 (2011) 1021.
[18] B. Bensmann, M. Petkovska, T. Vidakovic-Koch, R. Hanke-Rauschenbach, K. Sundmacher, J. Electrochem. Soc. 157 (2010) B1279.
[19] U. Krewer, A. Kamat, K. Sundmacher, J. Electroanal. Chem. 609 (2007) 105.
[20] P. Piela, T.E. Springer, J. Davey, P. Zelenay, J. Phys. Chem. C 111 (2007) 6512.
[21] U. Krewer, M. Christov, T. Vidakovic, K. Sundmacher, J. Electroanal. Chem. 589 (2006) 148.
[22] U. Krewer, H.K. Yoon, H.T. Kim, J. Power Sources 175 (2008) 760.
[23] G.R. Slone, The Audiophile's Project Sourcebook, McGraw-Hill/TAB Electronics, New York, 2001.
[24] J. Deseure, J. Power Sources 178 (2008) 323.
[25] U. Krewer, K. Sundmacher, J. Power Sources 154 (2005) 153.
[26] M.C. Tavares, S.A.S. Machado, L.H. Mazo, Electrochim. Acta 46 (2001) 4359.
[27] B.E. Conway, L. Bai, J. Electroanal. Chem. 198 (1986) 149.